TITLE: Functional rescue of dystrophin deficiency in mice caused by frameshift mutations using Campylobacter jejuni Cas9

AUTHORS: Koo, T; Lu-Nguyen, N B; Malerba, A; Kim, E; Kim, D; Cappellari, O; Cho, H-Y; Dickson, G; Popplewell, L; Kim, J-S

JOURNAL: Molecular Therapy

PUBLISHER: Elsevier

PUBLICATION DATE: April 2018 (online)

DOI: 10.1016/j.ymthe.2018.03.018

Royal
Veterinary
College
University of London

Functional rescue of dystrophin deficiency in mice caused by frameshift mutations using Campylobacter jejuni Cas9

Taeyoung Koo[1,2], Ngoc B Lu-Nguyen[3], Alberto Malerba[3], Eunji Kim[1], Daesik Kim[4], Ornella Cappellari[5], Hee-Yeon Cho[1], George Dickson[3], Linda Popplewell[3], and Jin-Soo Kim[1,2,4,*]

[1] Center for Genome Engineering, Institute for Basic Science (IBS), Seoul 08826, Republic of Korea

[2] Department of Basic Science, University of Science and Technology, Daejeon 34113, Republic of Korea

[3] Centre of Biomedical Sciences, School of Biological Sciences, Royal Holloway-University of London, Egham, Surrey, TW20 0EX, United Kingdom.

[4] Department of Chemistry, Seoul National University, Seoul 08826, Republic of Korea

[5] Comparative Biomedical Sciences, Royal Veterinary College, London, NW1 0TU, United Kingdom.

[*] Correspondence should be addressed to J.-S.K. (jskim01@snu.ac.kr)

ABSTRACT

Duchenne muscular dystrophy (DMD) is a fatal, X-linked muscle wasting disease caused by mutations in the *DMD* gene. In 51% of DMD cases, a reading frame is disrupted because of deletion of several exons. Here, we show that CjCas9 derived from *Campylobacter jejuni* can be used as a gene editing tool to correct an out-of-frame *Dmd* exon in *Dmd* knockout mice. Herein, we used Cas9 derived from *S. pyogenes* to generate *Dmd* knockout (KO) mice with a frameshift mutation in *Dmd* gene. Then, we expressed CjCas9, its single-guide RNA, and the eGFP gene in the *tibialis anterior* muscle of the *Dmd* KO mice using an all-in-one adeno-associated virus (AAV) vector. CjCas9 cleaved the target site in the *Dmd* gene efficiently *in vivo* and induced small insertions or deletions at the target site. This treatment resulted in conversion of the disrupted *Dmd* reading frame from out-of-frame to in-frame, leading to the expression of dystrophin in the sarcolemma. Importantly, muscle strength was enhanced in the CjCas9-treated muscles, without off-target mutations, indicating high efficiency and specificity of CjCas9. This work suggests that *in vivo DMD* frame correction, mediated by CjCas9 has great potential for the treatment of DMD and other neuromuscular diseases.

INTRODUCTION

Duchenne muscular dystrophy (DMD), an X-linked recessive disorder affecting 1 in 3,500 male births, is caused by nonsense or frameshift mutations in the gene encoding dystrophin, resulting in the absence of this protein in skeletal and cardiac muscles [1]. Dystrophin, an elongated protein localized to the inner face of the sarcolemma, is a key component in the assembly of the dystrophin-glycoprotein complex, which provides a mechanically strong link between the cytoskeleton and the extracellular matrix [2]. Dystrophin-deficient DMD muscle is therefore mechanically destabilized, a primary cause of the myofiber necrosis and muscle wasting associated with this lethal disease [3].

Conventional therapies are limited to supportive care that partially alleviates signs and symptoms, but does not directly target the disease mechanism, nor reverse the phenotype. Currently ongoing clinical trials include the following gene therapy strategies: dystrophin gene addition therapy using adeno-associated virus (AAV) vectors [4, 5]; cell transplantation therapy [6-8]; pharmacological rescue of *DMD* nonsense mutations [9, 10]; and exon skipping strategies to repair the *DMD* transcript reading frame [11-14]. There is currently only one approved drug (Eteplirsen) available for DMD using exon skipping strategy[15]. This approach is limited to specific mutations in addition to the requirement for repetitive administrations. Thus, new approaches are urgently needed.

Genome editing is a powerful method for creating permanent genetic modifications as a corrective treatment strategy for a variety of genetic diseases and as such could provide a means of gene therapy for DMD that that would only need to be administered once. In the context of DMD, gene editing has been achieved using programmable endonucleases, designed to specifically target a sequence of choice, to introduce a DNA double-strand break (DSB) in the genome. The *DMD* gene has been repaired either through efficient but error-prone non-homologous end joining (NHEJ) [16] or inefficient but precise homology-directed recombination (HDR) using a donor DNA template [17].

The power of these approaches has been dramatically increased by the development of the bacterial CRISPR/Cas9 system for correcting specific *DMD* mutations in both *ex vivo* and *in vivo* contexts [18-25]. In these studies, two different bacterial CRISPR-associated proteins have been tested: *Streptococcus pyogenes* Cas9 (SpCas9) [18, 21, 24] and *Staphylococcus aureus* Cas9 (SaCas9) [21-23]. To remove specific DMD-associated mutations, two intron-targeting sgRNAs together with SpCas9 or SaCas9 have been used to induce multiexon deletions in the *DMD* gene in human *DMD* patient cells [26] or single exon deletions in the *Dmd* gene which harbouring nonsense mutation. Both AAV vectors [18, 21-23] and adenoviral vectors [24] have been employed to

deliver the genome editing machinery *in vivo.* For the larger SpCas9, targeting efficacy was observed when the guide RNAs were delivered separately in a second AAV vector [23]. Due to the respective sizes of their coding sequences, SpCas9 (4.1 kbp) and SaCas9 (3.16 kbp) cannot be packaged into an AAV vector together with a single-guide (sg) RNA and a marker gene, which would allow tracking of delivery and expression *in vivo.* Very recently, the smallest Cas9 orthologue characterized to date (2.95 kb) was identified from *Campylobacter jejuni* [27] and packaged into an all-in-one AAV vector expressing CjCas9, sgRNA, and eGFP [28]. This vector has been successfully delivered into *tibialis anterior* (TA) muscles of C57BL/J wild-type mice, resulting in indel formation at the *Rosa26* locus with no detectable off-target effects up to 32 weeks post-injection [28]. Off-target mutations were rarely observed with CjCas9, partially because it has an extended protospacer-adjacent motif (PAM) (5'-NNNNRYAC-3') relative to SpCas9 (5'-NGG-3').

Approximately 51% of DMD patients harbour frameshifting exon deletions rather than point mutations, which are found in 27% of DMD patients based on the Leiden DMD mutation database[29]. Thus, the study was designed to demonstrate that introduction of double strand breaks into the genome could correct the disrupted reading frame of the *Dmd* gene harbouring frame shifting mutations. In this study, we investigated whether NHEJ-based genome editing using AAV-CjCas9 could correct the disrupted *Dmd* reading frame and restore a dystrophin protein expression to support muscle strength. We took advantage of the small size and target specificity of CjCas9 to package in an all-in-one AAV vector. We show here that NHEJ via a single AAV-CjCas9 delivery can repair an out-of-frame *Dmd* exon to in-frame sufficiently to restore *Dmd* muscle strength *in vivo.*

RESULTS

Generation of a *Dmd* KO mouse harboring a frameshift mutation

To investigate NHEJ-mediated repair of a disrupted *Dmd* reading frame, we generated a *Dmd* KO mouse via ribonucleoproteins (RNPs) delivery [30-32] of SpCas9 and a sgRNA targeting exon 23 of the *Dmd* gene (Figure 1A). Several of the resulting offspring displayed targeted mutations in the *Dmd* gene (Figure 1B). Sanger sequencing showed that *Dmd* mutations had occurred in 8 out of 31 offspring; all were heterozygous (Figure 1B, C). The male offspring showed no dystrophin protein expression (Figure 1D, E) as a result of the SpCas9-mediated frameshift mutation, indicating complete knockout (KO) of the *Dmd* gene.

Correction of the *Dmd* reading frame by CjCas9-mediated NHEJ

To investigate whether CjCas9 could restore the *Dmd* reading frame, we used CjCas9 and a 22 nucleotide-specific sgRNA [termed gX_{22} sgRNA, where "g" is an extra guanine nucleotide required for transcription under the control of the U6 promoter, targeting a region upstream of the premature stop codon (PSC) containing a 5'-NNNNGCAC-3' PAM in *Dmd* exon 23] (Figure 2A). The resulting construct was cloned into an all-in-one AAV vector plasmids and transfected in C2C12 myotubes. Indels were induced with a frequency of 25 ± 7.4% (Figure S1).

We next packaged sequences encoding CjCas9 and its sgRNA into a single AAV serotype 9 vector (Figure 2B). This AAV2/9-CjCas9 viral vector was administered via intramuscular injection into the TA muscles of 8 week old male *Dmd* KO mice (5×10^{11} vector genomes (v.g.) per TA muscle). CjCas9 induced indels with a frequency of 8 ± 0.7% or 3 ± 0.6% in TA muscles of *Dmd* KO mice harboring either the 1-bp insertion or the 14-bp deletion in exon 23, respectively, 8 weeks post-injection, as assessed by deep sequencing (Figure 2C). 27.2% of these indels caused the correction of the *Dmd* reading frame.

To determine the genome-wide specificity of the CjCas9 nuclease, nuclease-digested whole genome sequencing (Digenome-seq) [33-35] was used. In parallel, we tested SpCas9 nucleases (recognizing a 5'-NGG-3' PAM) that were designed to cleave sites that overlapped with the CjCas9 target sites. CjCas9 cleaved 8 sites in the mouse genome, whereas SpCas9 cleaved 105 sites (Figure 2D). Next, we performed targeted deep sequencing in AAV2/9-CjCas9 treated muscles at these potential Digenome-seq captured 8 off-target sites. No off-target indels were detectably induced at these off-target sites, whereas on-target indels were present with a frequency of 8 ± 0.7% in AAV2/9-CjCas9 treated TA muscles of *Dmd* KO mice harboring the 1-bp insertion mutation (Figure 2E and Table S1). It showed that the CjCas9 nuclease targeted the *Dmd* gene in skeletal muscles in a highly specific manner, without any detectable off-target effects *in vivo*.

Restoration of dystrophin protein expression that interacts with nNOS after CjCas9-mediated repair of the reading frame

Next, we examined whether the repaired *Dmd* reading frame led to dystrophin protein expression. The AAV2/9-CjCas9 delivery resulted in induction of dystrophin expression in TA muscles compared to that in the saline-injected control muscles (Figure 3A, *P* < 0.01). Approximately 39 ± 4% of the fibers were dystrophin positive in the 1-bp insertion mutation-

5

harboring *Dmd* KO mice with indel frequencies of 8 ± 0.7%, whereas 28 ± 6% of the fibers were dystrophin positive in the 14-bp deletion mutation-containing *Dmd* KO mice with indel frequencies of 3 ± 0.6% (Figure 3B). Dystrophin positive fibers showed sarcolemmal localization of neuronal nitric oxide synthase (nNOS) (Figure 3A). CjCas9 conjugated with HA tag was detected in the nucleus of dystrophin-positive fibers (Figure 3C). It was also detected at the sarcolemma of dystrophin positive myofibers, demonstrating the expression of CjCas9 in the fibers (Figure 3C).

Improvement of muscle strength in AAV2/9-CjCas9 treated muscles

To investigate the ability of the dystrophin protein induced by CjCas9-mediated NHEJ to increase muscle strength, AAV2/9-CjCas9 was injected into TA muscles of 8 week old male *Dmd* KO mice harboring the 14-bp deletion mutation (1 x 10^{12} v.g. /TA muscle) and *in situ* muscle physiology measurements were performed 7 weeks after injection. CjCas9 produced indels with a frequency of 2 ± 0.7 % (Figure 4A), corresponding to a increase in protein expression as observed by Western blot analysis (Figure 4B and Figure S2). In the CjCas9 edited muscles, 26 ± 4% of the fibers were dystrophin positive (Figure 4*C*).

Despite the low frequency of indels, dystrophin expression induced by CjCas9 led to an increase in specific maximal force in AAV2/9-CjCas9 treated muscles compared to saline-injected contralateral TA muscles from *Dmd* KO mice (*P< 0.01, ** *P*< 0.01, Figure 4D). Furthermore, AAV2/9-CjCas9 treated muscles did not show any difference in the maximal specific force at 180 Hz compared to wild-type TA muscles from C57BL/6 mice (Figure 4D).

DISCUSSION

This study provides the evidence that AAV2/9-CjCas9 delivered to dystrophic muscles leads to restoration of the disrupted reading frame via the introduction of indels upstream of the PSC with high efficiency and specificity. We observed dystrophin positive fibers interacting with neuronal nitric oxide synthase, supporting that the dystrophin protein functionally interacts with the dystrophin-associated protein complex in AAV2/9-CjCas9 injected muscles. In addition, muscle strength improvement was shown with indels induced at a frequency of 2% in the *Dmd* gene, suggesting that less than 2% reading frame correction is sufficient to induce a high level of dystrophin restoration that is correlated to an increase in dystrophic muscle strength.

The conventional exon deletion strategy used in previously reported CRISPR/Cas9-based studies for the treatment of DMD required dual guide RNAs to excise the exons [18, 21-24, 26]; an alternative strategy required a homology donor template to replace the nonsense mutation in the *mdx* mouse model [19, 21, 36]. In this study, we achieved NHEJ-mediated repair using CjCas9 and one sgRNA in the *Dmd* KO mouse harboring a frameshift mutation. The use of one rather than two sgRNAs has great advantages in terms of increasing targeting efficiency and avoiding the possibility of homologous recombination between the two U6 promoter-sgRNA sequences during viral DNA packaging in cells [37, 38]. Furthermore, a single AAV vector can be used to express Cas9 and its sgRNA, eliminating the need for two AAV vector systems.

In this study, targeted expression of CjCas9 and its sgRNA was achieved by the use of AAV serotype 9, which has tropism for skeletal and cardiac muscle [39], and, in the case of CjCas9, by the use of the SpC5-12 muscle-specific promoter. We linked the eGFP gene to the 3'-end of the CjCas9 gene with a T2A peptide sequence in between. This construct demonstrates the feasibility of adding other genetic elements in conjunction with CRISPR/Cas9 components to an all-in-one AAV vector. In addition, tracking of CjCas9-eGFP following systemic delivery into the whole mouse body should be applicable. Further development of CjCas9-mediated gene repair via HDR, in which missing exons in a donor template are inserted into *DMD*, may also contribute to the success of permanent gene correction with fully-functional, wild-type dystrophin protein expression.

Taken together, our findings show that application of all-in-one AAV-CjCas9 system is highly efficient in correcting the disrupted reading frame and improve the dystrophic muscle strength. This study should accelerate translation of gene editing therapeutic approaches to the clinical stage and holds great potential for DMD. This strategy is also particularly appealing for use in other frameshift mutation-associated neuromuscular diseases that exhibit lifelong progression.

MATERIALS AND METHODS

Animals. The care, use, and treatment of all animals in this study were in strict agreement with the ARVO statement for the Use of Animals in College of Veterinary Medicine and the guidelines established by the Seoul National University Institutional Animal Care and Use Committee (SNU-150130-2). Eight week old male, specific pathogen free (SPF) *Dmd* KO and C57BL6/J mice were used in this study. Mice were maintained under a 12 h dark–light cycle.

Generation of _Dmd_ KO mice. _Dmd_ knockout mice were generated by Macrogen, Inc. (Seoul, Korea) To generate male _Dmd_ mutants, a female pup (#14) heterozygous for a 1-bp insertion and a 14-bp deletion, both of which generated a premature stop codon (PSC) in _Dmd_ exon 23, was cross-bred with a C57/BL6J wild-type male mouse. Mice were interbred and maintained in pathogen-free conditions at Macrogen, Inc. All animal experiments were performed in accordance with Korean Food and Drug Administration (KFDA) guidelines. Protocols were reviewed and approved by the Institutional Animal Care and Use Committees (IACUC) of Macrogen, Inc. All manipulations were conducted with the approval of the Institutional Animal Care and Use Committee. Briefly, C57BL/6N female mice were treated with pregnant mare serum gonadotropin (PMSG) and human chorionic gonadotropin (HCG). After 48 hrs, these female mice were mated with C57BL/6N male mice. The next day, female mice containing vaginal plugs were sacrificed and fertilized embryos were harvested. A mixture of SpCas9 protein tagged with a nuclear localization signal and gRNAs targeting _Dmd_ exon 23 was microinjected into one-cell embryos. Microinjected embryos were incubated at 37℃ for 1-2 hrs, after which they were transplanted into the oviducts of pseudopregnant recipient mice.

Construction of AAV vector plasmid encoding CjCas9, its sgRNA, and eGFP. A human codon-optimized CjCas9-coding sequence, derived from _Campylobacter jejuni_ subsp. _Jejuni_ NCTC 11168, was modified by PCR to include a nuclear localization signal (NLS) and an HA epitope, as well as self-cleaving T2A peptide and enhanced green fluorescent protein (eGFP) sequences at its 3'-end. The resulting sequence was cloned into the AAV inverted terminal repeat-based vector plasmid. The trans-activating crRNA (tracrRNA) sequence and the precursor CRISPR RNA (pre-crRNA) sequence were fused with a TGAA linker to form a sgRNA sequence [28]. _Dmd_ exon 23 targeting sgRNAs were transcribed under the control of the U6 promoter and CjCas9 expression was controlled by the by the synthetic muscle-specific SPc5-12 promoter [40] in C2C12 myoblast cells and mouse TA muscles.

Cell culture and transfection of AAV vector plasmids. C2C12 (ATCC, CRL-1772) myoblast cells were maintained in Dulbecco's Modified Eagle's Medium (DMEM, Welgene, cat. no. LM001-05) supplemented with 100 units per ml penicillin (Gibco, cat. no. 15140-122), 100 mg/ml streptomycin, and 10% fetal bovine serum heat-inactivated (FBS, Welgene, cat. no. S 101-01). AAV vector plasmids expressing sgRNA and CjCas9 were transfected into cells with lipofectamine 2000 (Invitrogen, cat. no. 11668019); cells were maintained in DMEM

supplemented with 2% FBS for differentiation. After 5 days of transfection, genomic DNA was isolated using a DNeasy Blood & Tissue kit (Qiagen, cat. no. 69581).

Production and titration of AAV vectors. To produce AAV vectors, they were pseudotyped in AAV9 rep/cap capsids (pAAV2/9). HEK293T cells (ATCC, CRL-3216) were transfected with pAAV-ITR-CjCas9-sgRNA, pAAV2/9 encoding for AAV2rep and AAV9cap, and helper plasmid. HEK293T cells were cultured in DMEM with 2% FBS. Recombinant pseudotyped AAV vector stocks were generated using PEI coprecipitation with PEIpro (Polyplus-transfection) and triple-transfection with plasmids at a molar ratio of 1:1:1 in HEK293T cells. After 72 h of incubation, cells were lysed and particles were purified by iodixanol (Sigma-Aldrich) step-gradient ultracentrifugation. The number of vector genomes was determined by quantitative PCR.

Intramuscular injection of AAV. Intramuscular delivery of 5×10^{11} vg to 1×10^{12} vg of vector in physiological saline (40 μl) was performed via longitudinal injection into *tibialis anterior* (TA) muscles of 8-week-old male Dmd-knockout mice anesthetized with 2–4% isoflurane. Muscles were injected using an ultra-fine insulin syringe with a 31G needle (BD). As a negative control, C57BL/6J and *Dmd* KO mice were injected with physiological saline only. We used 40 μl of AAV to deliver AAV to whole TA muscles. To confirm the injection target, the corresponding tendon *reflexes* were carefully checked.

Genomic DNA extraction and mutation analysis. Muscle tissue was homogenized using tungsten carbide beads (3mm; Qiagen) and a TissueLyser II (Qiagen). Genomic DNA was isolated from the homogenized tissue using a NucleoSpin Tissue kit (Macherey-Nagel). On-target or off-target loci were amplified using 100 ng of genomic DNA for targeted deep sequencing. Deep sequencing libraries were generated by PCR with the following primers: *Dmd* exon 23, 5'-CTCATCAAATATGCGTGTTAGTGT-3' (forward), 5'-CACCAACTGGGAGGAAAGTT-3' (reverse). TruSeq HT Dual index primers were used to label each sample. Pooled libraries were subjected to paired-end sequencing using MiniSeq (Illumina). Indel frequencies were calculated as described previously [33].

Digenome sequencing. Digenome-seq was performed as described previously [33, 34]. Genomic DNA was isolated using a DNeasy Blood & Tissue kit (Qiagen) according to the manufacturer's instructions. Genomic DNA isolated from muscles of C57BL/6J mice (8 μg) was mixed with CjCas9 or SpCas9 protein (300nM) and sgRNA (900nM) in a 400 μl reaction volume (100 mM

NaCl, 50 mM Tris-HCl, 10 mM MgCl2, and 100 µg/ml BSA) and the mixture was incubated for 8h at 37 ℃. Digested genomic DNA was then incubate d with RNase A (50 µg/ml) for 30 min at 37 ℃ and purified again with a DNeasy Blood & Tiss ue kit (Qiagen). Digested DNA was fragmented using the Covaris system and ligated with adaptors for library formation. DNA libraries were subjected to whole-genome-sequencing (WGS) using an Illumina HiSeq X Ten Sequencer at Macrogen. We used the Isaac aligner to generate a Bam file using the following parameters: ver. 01.14.03.12; Mouse genome reference, mm10 from UCSC; Base quality cutoff, 15; Keep duplicate reads, yes; Variable read length support, yes; Realign gaps, no; and Adaptor clipping, yes (adaptor: AGATCGGAAGAGC*, *GCTCTTCCGATCT) [41]. A DNA cleavage score was assigned to each nucleotide position across the entire genome, using WGS data, according to the equation presented in Kim *et al*[34]. *In vitro* cleavage sites with DNA cleavage scores above the cut-off value of 2.5 were computationally identified.

Immunofluorescent staining and imaging of tissue. TA muscles were excised from tendon to tendon, and OCT embedded samples were rapidly frozen in liquid nitrogen-cooled isopentane. To assess muscle pathology, 10-mm cryosections were prepared. Cross-section samples were immunostained with anti-dystrophin antibody (Abcam, 15277), anti-laminin antibody (Sigma, L0663), anti-HA tag antibody (Abcam, ab9110), and Alexa Fluor 594 (Invitrogen, A11037) or Alexa Fluor 488 antibodies (Invitrogen, A11006, A11039). Muscle sections were imaged using a standard fluorescence (Nikon Eclipse Ti) microscope and a confocal microscope (LSM 710, Carl Zeiss). The scanning parameters were as follows: scaling (x = 0.208 µm/pixel, y = 0.208 µm/pixel), dimensions (x = 106.07 µm, y = 106.07 µm, channels: 4, 12-bit) with objective C-Apochromat 80x/1.20W Korr M27. ZEN 2009 software was used to process the images. To track the expression of CjCas9, HA tag conjugated CjCas9 was visualized under confocal microscopy. Quantification of dystrophin-positive myofibers in muscle cross-sectional area was performed via counting the dystrophin expressing fibers in 844 to 1,182 individual myofibers per TA using Adobe Photoshop (n=5 TAs per treatment group). The percentage of dystrophin expressing fibers was calculated by dividing the number of dystrophin positive fibers by the number of laminin expressing fibers (a measure of the total number of fibers) and multiplying by 100. Sample randomization was done in this analysis".

Western blotting. Muscles were homogenized in 300 µl of homogenization buffer (ThermoFisher, 89900). Protein extracted from the C57BL/6 muscles were loaded at 10%, 5% and 1% of total protein (30 µg), whereas 30 µg of protein was loaded in the AAV-treated and

mock control group. Thus, the band for GAPDH represents the corresponding protein loading of the samples. Proteins were separated on a 3%-8% polyacrylamide Tris-acetate gel (Invitrogen) and transferred onto a 0.2 μm nitrocellulose membrane (Hybond ECL membrane; Amersham Biosciences). Dystrophin was detected using rabbit anti-dystrophin antibodies (Abcam, ab15277); GAPDH was detected with anti-GAPDH antibodies (Abcam, ab9485) as an internal control. The membrane was incubated with primary antibodies at room temperature for 1 hr. Goat anti-rabbit IgG-HRP antibody (Abcam, ab6721) was used for signal detection. The membrane was exposed to SuperSignal West Pico Chemiluminescent Substrate (Cat.no NC14080KR) and Ez-Capture MG (ATTO) was used for digital imaging. The experiments were repeated three times, and representative results performed in duplicate are shown in this study.

In vivo **force measurements.** Seven weeks after AAV2/9-CjCas9 injection, the function of both TA muscles from each mouse was assessed. This procedure was adapted from standard protocols [42, 43] and has been previously described [44]. Mice were deeply anesthetized and were carefully monitored throughout the experiment to ensure that there was no reflex response to toe pinch. The distal tendon of the TA muscle was dissected from surrounding tissue and tied with 4.0 braided surgical silk (Interfocus, Cambridge, UK). The sciatic nerve was exposed and superfluous branches axotomized, leaving the TA motor innervation via the common peroneal nerve intact. The foot was secured to a platform and the ankle and knee immobilized using stainless steel pins. The TA tendon was attached to the lever arm of a 305B dual-mode servomotor transducer (Aurora Scientific, Aurora, Ontario, Canada) via a custom made steel s-hook. TA muscle contractions were elicited by stimulating the distal part of common peroneal nerve via bipolar platinum electrodes, using supramaximal square-wave pulses of 0.02 ms (701A stimulator; Aurora Scientific). Data were acquired and the servomotors controlled using a Lab-View-based DMC program (Dynamic muscle control and Data Acquisition; Aurora Scientific). Optimal muscle length (Lo) was determined by incrementally stretching the muscle using micromanipulators until the maximum isometric twitch force was achieved. Maximum isometric tetanic force (Po) was determined from the plateau of the force–frequency relationship following a series of stimulations at 10, 30, 40, 50, 80, 100, 120, 150, and 180 Hz. A 1-min rest period was allowed between each tetanic contraction. The specific force (N/cm^2) was calculated by dividing Po by the TA muscle cross-sectional area. The overall cross-sectional area was estimated using the following formula: muscle weight (g)/[TA fiber length (Lf; cm) × 1.06 (g/cm^3)].

Statistical analysis. No statistical methods were used to predetermine sample size for *in vitro* or *in vivo* experiments. To avoid scientific bias we randomized the mice from different litters for the *in vivo* experiments before injections. Furthermore, scientists were blinded to the samples during analysis of dystrophin quantification and during muscle strength assessment by electrophysiology. All group results are expressed as mean ± SEM. Comparisons between groups were made using the one-way ANOVA with *Tukey*'s post-hoc tests. Statistical significance as compared to untreated controls is denoted with * ($P < 0.05$), ** ($P < 0.01$), *** ($P < 0.001$), ns; not significant in the figures and figure legends. Statistical analysis was performed in Graph Pad PRISM 5.

ACCESSION NUMBER

The deep sequencing data from this study have been submitted to the NCBI Sequence Read Archive (http://www.ncbi.nlm.nih.gov/sra) under accession number SRP131242.

SUPPLEMENTARY DATA

Supplementary Data are available at Online.

FUNDING

Conflict of interest statement. J.-S.K. is a co-founder and shareholder of ToolGen, Inc and E.K. have filed patent applications. The remaining authors declare no competing financial interests.

Authors' contributions

T.K., P.L., G.D., and J.-S.K. supervised the research. T.K. and all the other authors performed the experiments. T.K., P.L., and A.M. wrote the manuscript and G.D. and J.-S.K critically editing it with comments. All authors read and approved the final manuscript.

REFERENCES

1. Muntoni, F, Torelli, S, and Ferlini, A (2003). Dystrophin and mutations: one gene, several proteins, multiple phenotypes. *Lancet Neurol* **2**: 731-740.
2. Gumerson, JD, and Michele, DE (2011). The dystrophin-glycoprotein complex in the prevention of muscle damage. *J Biomed Biotechnol* **2011**: 210797.

3.   Culligan, KG, Mackey, AJ, Finn, DM, Maguire, PB, and Ohlendieck, K (1998). Role of dystrophin isoforms and associated proteins in muscular dystrophy (review). *Int J Mol Med* **2**: 639-648.

4.   Blankinship, MJ, Gregorevic, P, and Chamberlain, JS (2006). Gene therapy strategies for Duchenne muscular dystrophy utilizing recombinant adeno-associated virus vectors. *Mol Ther* **13**: 241-249.

5.   Mendell, JR, Campbell, K, Rodino-Klapac, L, Sahenk, Z, Shilling, C, Lewis, S*, et al.* (2010). Dystrophin immunity in Duchenne's muscular dystrophy. *N Engl J Med* **363**: 1429-1437.

6.   Skuk, D, Goulet, M, Roy, B, Chapdelaine, P, Bouchard, JP, Roy, R*, et al.* (2006). Dystrophin expression in muscles of duchenne muscular dystrophy patients after high-density injections of normal myogenic cells. *J Neuropathol Exp Neurol* **65**: 371-386.

7.   Skuk, D, Goulet, M, Roy, B, Piette, V, Cote, CH, Chapdelaine, P*, et al.* (2007). First test of a "high-density injection" protocol for myogenic cell transplantation throughout large volumes of muscles in a Duchenne muscular dystrophy patient: eighteen months follow-up. *Neuromuscul Disord* **17**: 38-46.

8.   Torrente, Y, Belicchi, M, Marchesi, C, D'Antona, G, Cogiamanian, F, Pisati, F*, et al.* (2007). Autologous transplantation of muscle-derived CD133+ stem cells in Duchenne muscle patients. *Cell Transplant* **16**: 563-577.

9.   Bushby, K, Finkel, R, Wong, B, Barohn, R, Campbell, C, Comi, GP*, et al.* (2014). Ataluren treatment of patients with nonsense mutation dystrophinopathy. *Muscle Nerve* **50**: 477-487.

10.   Finkel, RS, Flanigan, KM, Wong, B, Bonnemann, C, Sampson, J, Sweeney, HL*, et al.* (2013). Phase 2a study of ataluren-mediated dystrophin production in patients with nonsense mutation Duchenne muscular dystrophy. *PLoS One* **8**: e81302.

11.   Goemans, NM, Tulinius, M, van den Akker, JT, Burm, BE, Ekhart, PF, Heuvelmans, N*, et al.* (2011). Systemic administration of PRO051 in Duchenne's muscular dystrophy. *N Engl J Med* **364**: 1513-1522.

12.   Kinali, M, Arechavala-Gomeza, V, Feng, L, Cirak, S, Hunt, D, Adkin, C*, et al.* (2009). Local restoration of dystrophin expression with the morpholino oligomer AVI-4658 in Duchenne muscular dystrophy: a single-blind, placebo-controlled, dose-escalation, proof-of-concept study. *Lancet Neurol* **8**: 918-928.

13.   van Deutekom, JC, Janson, AA, Ginjaar, IB, Frankhuizen, WS, Aartsma-Rus, A, Bremmer-Bout, M*, et al.* (2007). Local dystrophin restoration with antisense oligonucleotide PRO051. *N Engl J Med* **357**: 2677-2686.

14.   Cirak, S, Arechavala-Gomeza, V, Guglieri, M, Feng, L, Torelli, S, Anthony, K*, et al.* (2011). Exon skipping and dystrophin restoration in patients with Duchenne muscular dystrophy after systemic phosphorodiamidate morpholino oligomer treatment: an open-label, phase 2, dose-escalation study. *Lancet* **378**: 595-605.

15.   Mendell, JR, Goemans, N, Lowes, LP, Alfano, LN, Berry, K, Shao, J*, et al.* (2016). Longitudinal effect of eteplirsen versus historical control on ambulation in Duchenne muscular dystrophy. *Ann Neurol* **79**: 257-271.

16.   Chapdelaine, P, Pichavant, C, Rousseau, J, Paques, F, and Tremblay, JP (2010). Meganucleases can restore the reading frame of a mutated dystrophin. *Gene Ther* **17**: 846-858.

17.   Popplewell, L, Koo, T, Leclerc, X, Duclert, A, Mamchaoui, K, Gouble, A*, et al.* (2013). Gene correction of a duchenne muscular dystrophy mutation by meganuclease-enhanced exon knock-in. *Hum Gene Ther* **24**: 692-701.

18.   Long, C, Amoasii, L, Mireault, AA, McAnally, JR, Li, H, Sanchez-Ortiz, E*, et al.* (2016). Postnatal genome editing partially restores dystrophin expression in a mouse model of muscular dystrophy. *Science* **351**: 400-403.

19. Long, C, McAnally, JR, Shelton, JM, Mireault, AA, Bassel-Duby, R, and Olson, EN (2014). Prevention of muscular dystrophy in mice by CRISPR/Cas9-mediated editing of germline DNA. *Science* **345**: 1184-1188.

20. Ousterout, DG, Kabadi, AM, Thakore, PI, Perez-Pinera, P, Brown, MT, Majoros, WH*, et al.* (2015). Correction of dystrophin expression in cells from Duchenne muscular dystrophy patients through genomic excision of exon 51 by zinc finger nucleases. *Mol Ther* **23**: 523-532.

21. Bengtsson, NE, Hall, JK, Odom, GL, Phelps, MP, Andrus, CR, Hawkins, RD*, et al.* (2017). Muscle-specific CRISPR/Cas9 dystrophin gene editing ameliorates pathophysiology in a mouse model for Duchenne muscular dystrophy. *Nat Commun* **8**: 14454.

22. Nelson, CE, Hakim, CH, Ousterout, DG, Thakore, PI, Moreb, EA, Castellanos Rivera, RM*, et al.* (2016). In vivo genome editing improves muscle function in a mouse model of Duchenne muscular dystrophy. *Science* **351**: 403-407.

23. Tabebordbar, M, Zhu, K, Cheng, JK, Chew, WL, Widrick, JJ, Yan, WX*, et al.* (2016). In vivo gene editing in dystrophic mouse muscle and muscle stem cells. *Science* **351**: 407-411.

24. Xu, L, Park, KH, Zhao, L, Xu, J, El Refaey, M, Gao, Y*, et al.* (2016). CRISPR-mediated Genome Editing Restores Dystrophin Expression and Function in mdx Mice. *Mol Ther* **24**: 564-569.

25. Young, CS, Hicks, MR, Ermolova, NV, Nakano, H, Jan, M, Younesi, S*, et al.* (2016). A Single CRISPR-Cas9 Deletion Strategy that Targets the Majority of DMD Patients Restores Dystrophin Function in hiPSC-Derived Muscle Cells. *Cell Stem Cell* **18**: 533-540.

26. Ousterout, DG, Kabadi, AM, Thakore, PI, Majoros, WH, Reddy, TE, and Gersbach, CA (2015). Multiplex CRISPR/Cas9-based genome editing for correction of dystrophin mutations that cause Duchenne muscular dystrophy. *Nat Commun* **6**: 6244.

27. Fonfara, I, Le Rhun, A, Chylinski, K, Makarova, KS, Lecrivain, AL, Bzdrenga, J*, et al.* (2014). Phylogeny of Cas9 determines functional exchangeability of dual-RNA and Cas9 among orthologous type II CRISPR-Cas systems. *Nucleic Acids Res* **42**: 2577-2590.

28. Kim, E, Koo, T, Park, SW, Kim, D, Kim, K, Cho, HY*, et al.* (2017). In vivo genome editing with a small Cas9 orthologue derived from Campylobacter jejuni. *Nat Commun* **8**: 14500.

29. Aartsma-Rus, A, Fokkema, I, Verschuuren, J, Ginjaar, I, van Deutekom, J, van Ommen, GJ*, et al.* (2009). Theoretic applicability of antisense-mediated exon skipping for Duchenne muscular dystrophy mutations. *Hum Mutat* **30**: 293-299.

30. Kim, S, Kim, D, Cho, SW, Kim, J, and Kim, JS (2014). Highly efficient RNA-guided genome editing in human cells via delivery of purified Cas9 ribonucleoproteins. *Genome Res* **24**: 1012-1019.

31. Cho, SW, Lee, J, Carroll, D, Kim, JS, and Lee, J (2013). Heritable gene knockout in Caenorhabditis elegans by direct injection of Cas9-sgRNA ribonucleoproteins. *Genetics* **195**: 1177-1180.

32. Sung, YH, Kim, JM, Kim, HT, Lee, J, Jeon, J, Jin, Y*, et al.* (2014). Highly efficient gene knockout in mice and zebrafish with RNA-guided endonucleases. *Genome Res* **24**: 125-131.

33. Kim, D, Bae, S, Park, J, Kim, E, Kim, S, Yu, HR*, et al.* (2015). Digenome-seq: genome-wide profiling of CRISPR-Cas9 off-target effects in human cells. *Nat Methods* **12**: 237-243, 231 p following 243.

34. Kim, D, Kim, S, Kim, S, Park, J, and Kim, JS (2016). Genome-wide target specificities of CRISPR-Cas9 nucleases revealed by multiplex Digenome-seq. *Genome Res* **26**: 406-415.

35. Kim, D, Kim, J, Hur, JK, Been, KW, Yoon, SH, and Kim, JS (2016). Genome-wide analysis reveals specificities of Cpf1 endonucleases in human cells. *Nat Biotechnol* **34**: 863-868.

36. Li, HL, Fujimoto, N, Sasakawa, N, Shirai, S, Ohkame, T, Sakuma, T*, et al.* (2015). Precise correction of the dystrophin gene in duchenne muscular dystrophy patient induced pluripotent stem cells by TALEN and CRISPR-Cas9. *Stem Cell Reports* **4**: 143-154.

37. Wright, JF (2008). Manufacturing and characterizing AAV-based vectors for use in clinical studies. *Gene Ther* **15**: 840-848.

38. Allen, JM, Debelak, DJ, Reynolds, TC, and Miller, AD (1997). Identification and elimination of replication-competent adeno-associated virus (AAV) that can arise by nonhomologous recombination during AAV vector production. *J Virol* **71**: 6816-6822.

39. Zincarelli, C, Soltys, S, Rengo, G, and Rabinowitz, JE (2008). Analysis of AAV serotypes 1-9 mediated gene expression and tropism in mice after systemic injection. *Mol Ther* **16**: 1073-1080.

40. Li, X, Eastman, EM, Schwartz, RJ, and Draghia-Akli, R (1999). Synthetic muscle promoters: activities exceeding naturally occurring regulatory sequences. *Nat Biotechnol* **17**: 241-245.

41. Raczy, C, Petrovski, R, Saunders, CT, Chorny, I, Kruglyak, S, Margulies, EH*, et al.* (2013). Isaac: ultra-fast whole-genome secondary analysis on Illumina sequencing platforms. *Bioinformatics* **29**: 2041-2043.

42. Liu, M, Yue, Y, Harper, SQ, Grange, RW, Chamberlain, JS, and Duan, D (2005). Adeno-associated virus-mediated microdystrophin expression protects young mdx muscle from contraction-induced injury. *Mol Ther* **11**: 245-256.

43. Sharp, PS, Dick, JR, and Greensmith, L (2005). The effect of peripheral nerve injury on disease progression in the SOD1(G93A) mouse model of amyotrophic lateral sclerosis. *Neuroscience* **130**: 897-910.

44. Foster, H, Sharp, PS, Athanasopoulos, T, Trollet, C, Graham, IR, Foster, K*, et al.* (2008). Codon and mRNA sequence optimization of microdystrophin transgenes improves expression and physiological outcome in dystrophic mdx mice following AAV2/8 gene transfer. *Mol Ther* **16**: 1825-1832.

Figure legends

Figure 1. Generation of a *Dmd* KO mouse. (A) SpCas9 target sequence in exon 23 of the murine *Dmd* gene. The PAM sequence of SpCas9 is shown in red and the target sequence in blue. The predicted Cas9 cleavage site is marked by a red arrowhead. (B) Sanger sequencing assay to analyze mutations at the target site. The numbers of offspring obtained after transplant into surrogate mothers and mutants generated are indicated. Inserted nucleotides are shown in yellow**.** (C) Mutations at the target site in offspring from an F0 mouse (#14) cross-bred with a C57BL/6 wild-type mouse. The male offspring harbors either a 1-bp insertion mutation (1-bp ins) or a 14-bp deletion (14-bp del) mutation at the *Dmd* exon 23 site, generating a frameshift to be targeted by CjCas9. The PAM sequence of CjCas9 is shown in green and the target sequence in orange. Predicted CjCas9 cleavage sites are marked by red arrowheads. (D) Western blot

analysis of extracts from TA muscles from wild-type (WT) and *Dmd* KO mice (14-bp del and 1-bp ins) to detect dystrophin and GAPDH protein (control). (E) Histological analysis of TA muscles from wild-type and Dmd KO mice (14-bp del and 1-bp ins). Dystrophin and laminin (control) are shown in red and green, respectively.

Figure 2. *In vivo* genome editing with CjCas9 in TA muscles of *Dmd* KO mice. (A) SpCas9 and CjCas9 target sequences in exon 23 of the murine *Dmd* gene. Predicted Cas9 cleavage sites are marked by red arrowheads. PSC; premature stop codon. (B) Schematic diagram of the all-in-one AAV vector encoding the sgRNA and CjCas9 conjugated to eGFP. (C) Indel frequencies (left) and representative mutant sequences (right) at the *Dmd* target site in TA muscles of *Dmd* KO mice (1-bp ins and 14-bp del) 8 weeks after injection with AAV2/9-CjCas9. (Right) The inserted nucleotide in *Dmd* KO mice harboring a 1-bp ins is shown in blue, the target sequence in orange, and the PAM sequence in green; the number of deleted bases is shown on the right. Error bars are shown as mean ± S.E.M (n=3). (D) Digenome-seq analysis. The Circos plot shows genome-wide DNA cleavage scores across the mouse genome. The red arrow indicates the on-target sites for CjCas9 (orange) or SpCas9 (blue). (Bottom) The target sites for SpCas9 and CjCas9 at the *Dmd* locus are indicated by the blue and orange lines, respectively. The numbers of in vitro cleavage sites identified by Digenome-seq for the two enzymes are indicated. (E) Indel frequencies at Digenome-seq captured off-target sites. On; on-target site, OTS; off-target site. Mismatched nucleotides are shown in red and PAM sequences of CjCas9 in green. The red arrow indicates cleavage positions within the 22-bp target sequences. Error bars are shown as mean ± S.E.M (n=3~4).

Figure 3. CjCas9 mediated dystrophin correction interacts with the dystrophin-associated protein complex. (A) Histological analysis of TA muscles from wild-type and *Dmd* KO mice (1-bp ins and 14-bp del) 8 weeks after treatment with AAV2/9-CjCas9. The white stars indicate the same muscle fiber in dystrophin- and nNOS-stained sections. (B) Quantification of dystrophin positive fibers in TA muscle cross sections. Error bars are shown as mean ± S.E.M (n=3). (C) Representative confocal images of dystrophin and HA-tag expression as a proxy for CjCas9 expression in TA muscle from mice treated with AAV2/9-CjCas9.

Figure 4. Gene editing increases muscle strength. (A) Indel frequencies at the *Dmd* target site in TA muscles from *Dmd* KO mice (14-bp del) 7 weeks after intramuscular injection of

16

AAV2/9-CjCas9. Error bars are shown as mean ± S.E.M (n=5). (B) Western blot analysis of TA muscle samples from wild-type mice, *Dmd* KO mice (14-bp del), and AAV2/9-CjCas9 treated *Dmd* KO mice to detect dystrophin and GAPDH protein. (C) (Left) Histological analysis of TA muscles from wild-type and *Dmd* KO mice treated with AAV2/9-CjCas9. (Right) Quantification of dystrophin positive fibers in cross sections of TA muscle from *Dmd* KO mice harboring the 14-bp deletion mutation. Error bars are shown as mean ± S.E.M (n=5). (D) The specific force (mN/cm^2) generated by the TA muscle. Error bars are shown as mean ±S.E.M (n=4).

Figure 1

A

exon22　exon23　exon24

sgRNA

```
5'-ACCTTCAGAAATATGCCAGAAATATCTGTCAGAATTTGAAGAGATTGAG-3'
3'-TGGAAGTCTTTATACGGTCTTTATAGACAGTCTTAAACTTCTCTAACTC-5'
```

B

Target gene	No. of offspring	Mutant ratio (%)
DMD	31	26 (8/31)

```
WT   CTCAATCTCTTCAAATTCTGACAGATATTTCTGGCATATTTC-TGAAGGTGCTTTCTTGGCCATCTCCTTCACA
#5   CTCAATCTCTTCAAATTCTGACAGATATTTC------------TGAAGGTGCTTTCTTGGCCATCTCCTTCACA   -11
     CTCAATCTCTTCAAATTCTGACAGATATTTCT--------------GGTGCTTTCTTGGCCATCTCCTTCACA   -14
#7   CTCAATCTCTTCAAATTCTGACAGATATTTCTGGCATATTTC-TGAAGGTGCTTTCTTGGCCATCTCCTTCACA   WT
     CTCAATCTCTTCAAATTCTGACAGATATTTCTG---------------GCTTTCTTGGCCATCTCCTTCACA   -16
#9   CTCAATCTCTTCAAATTCTGACAGATATTTCTG------------------GCTTTCTTGGCCATCTCCTTCACA   -16
     CTCAATCTCTTCAAATTCTGACAGATATTTCTGGCC----------------TTCTTGGCCATCTCCTTCACA   -16
#10  CTCAATCTCTTCAAATTCTGACAGATATTTCTGG----------GAAGGTGCTTTCTTGGCCATCTCCTTCACA   -9
     CTCAATCTCTTCAAATTCTGACAGATATTTCTGGCATA--TC-TGAAGGTGCTTTCTTGGCCATCTCCTTCACA   -2
#14  CTCAATCTCTTCAAATTCTGACAGATATTTCTGGCATATTTCGTGAAGGTGCTTTCTTGGCCATCTCCTTCACA   +1
     CTCAATCTCTTCAAATTCTGACAGATATTTCT--------------GGTGCTTTCTTGGCCATCTCCTTCACA   -14
#15  CTCAATCTCTTCAAATTCTGACAGATATTTCTGGCATATTTA-TGAAGGTGCTTTCTTGGCCATCTCCTTCACA   0
     CTCAATCTCTTCAAATTCTGACAGATATTTCTGGCATATTTC-TGAAGGTGCTTTCTTGGCCATCTCCTTCACA   WT
#22  CTCAATCTCTTCAAATTCTGACAGATATTTCTGGCATATTT--TGAAGGTGCTTTCTTGGCCATCTCCTTCACA   -1
     CTCAATCTCTTCAAATTCTGACAGATATTTCTGGCATATTTC---------CTTTCTTGGCCATCTCCTTCACA   -8
     CTCAATCTCTTCAAATTCTGACAGATATTTCTGGCATATTTCTTGAAGGTGCTTTCTTGGCCATCTCCTTCACA   +1
#26  CTCAATCTCTTCAAATTCTGACAGATATTTCT--------------GGTGCTTTCTTGGCCATCTCCTTCACA   -14
```

C

Dmd-KO mice (14-bp del)
```
5'-GACACTGTGAAGGAGATGGCCAAGAAAGCACC---------------AGA-3'
3'-CTGTGACACTTCCTCTACCGGTTCTTTCGTGG---------------TCT-5'
```

Dmd-KO mice (1-bp ins)
```
5'-GACACTGTGAAGGAGATGGCCAAGAAAGCACCCTTCACGAAATATGCCAGA-3'
3'-CTGTGACACTTCCTCTACCGGTTCTTTCGTGGAAGTGCTTTATACGGTCT-5'
```

D

| | Ladder | WT | | | Dmd KO | |
| | | 10% | 5% | 1% | 14-bp del | 1-bp ins |

460kDa — Dystrophin

41kDa
31kDa — GAPDH

E

	Dystrophin	Laminin
WT		
Dmd KO (14-bp del)		
Dmd KO (1-bp ins)		

Figure 2

A

CjCas9

PSC

5'-GACACTGTGAAGGAGATGGCCAA**GAAAGCAC**CTTCAGAAATATGCCAGAAATATCTGTCAGAATT**TGA**AGAGA-3'

3'-CTGTGACACTTCCTCTACCGGTTCTTTCGT**GGA****AGTCTTTATACGGTCTTTA**TAGACAGTCTTAAACTTCTCT-5'

SpCas9

B

ITR — U6 — sgRNA — Spc5-12 — *CjCas9* — NLS HA tag — eGFP — polyA — ITR

4825-bp

C

Indels (%) chart with y-axis 0–10, categories:
- -AAV (1-bp ins)
- +AAV (1-bp ins)
- -AAV (14-bp del)
- +AAV (14-bp del)
** significance

```
GTGACACTGTGAAGGAGATGGCCAAGAAAGCACCTTCACGAAATATGCCA  1-bp ins
GTGACACTGTGAAGGAGATGGC--AGAAAGCACCTTCACGAAATATGCCA  (-2)
GTGACACTGTGAAGGAGATGGC-AAGAAAGCACCTTCACGAAATATGCCA  (-1)
GTGACACTGTGAAGGAGAT---CAAGAAAGCACCTTCACGAAATATGCCA  (-3)
GTGACACTGTGAAGGAGATGGC----AAAGCACCTTCACGAAATATGCCA  (-4)
GTGACACTGTGAAGGAGATGGC---GAAAGCACCTTCACGAAATATGCCA  (-3)

GTGACACTGTGAAGGAGATGGCCAAGAAAGCACC--------------AG  14-bp del
GTGACACTGTGAAGGAGATGGC----AAAGCACC--------------AG  (-4)
GTGACACTGTGAAGGAGATGGC--AGAAAGCACC--------------AG  (-2)
GTGACACTGTGAAGGAG-----CAAGAAAGCACC--------------AG  (-5)
GTGACACTGTGAAGGAGATGG-CAAGAAAGCACC--------------AG  (-1)
GTGACACTGT---------------AGCACC--------------AG  (-18)
```

D

On-target

(-) Nuclease   (+) SpCas9   (+) CjCas9

CjCas9

Dmd 5'-CTATCTGAGTGACACTGTGA**AGG**AGATGGCCAA**GAAAGCAC**-3'

SpCas9

	SpCas9	CjCas9
	105	8

E


```
cCgtgtTctAaGgagatGCCAATGAGACAC  OTS8   <0.001
ACgaTaTagAaGgagatGaCAAAGAAACAC  OTS7   <0.001
gCtggGgtgAaGgagatGCCAAGAACACAC  OTS6   <0.001 / <0.001
cataaagGAAGaAGAcaGCCAACTCCACAC  OTS5   <0.001 / <0.001
caggcaaaAAGGAGAaaGCCAACTGAACAC  OTS4   <0.001
caAgTtgGAAGGAGAgaGCCAAGTCCACAC  OTS3
AtAagtcaAAAaGgagatGgCAATTCAACAC OTS2   <0.001 / <0.001
AaagatgGAAGGAGAaaGCCAATTCCACAC  OTS1   <0.001 / <0.001
ACACTGTGAAGGAGATGGCCAAGAAAGCAC  On     <0.001
```

+AAV (black)
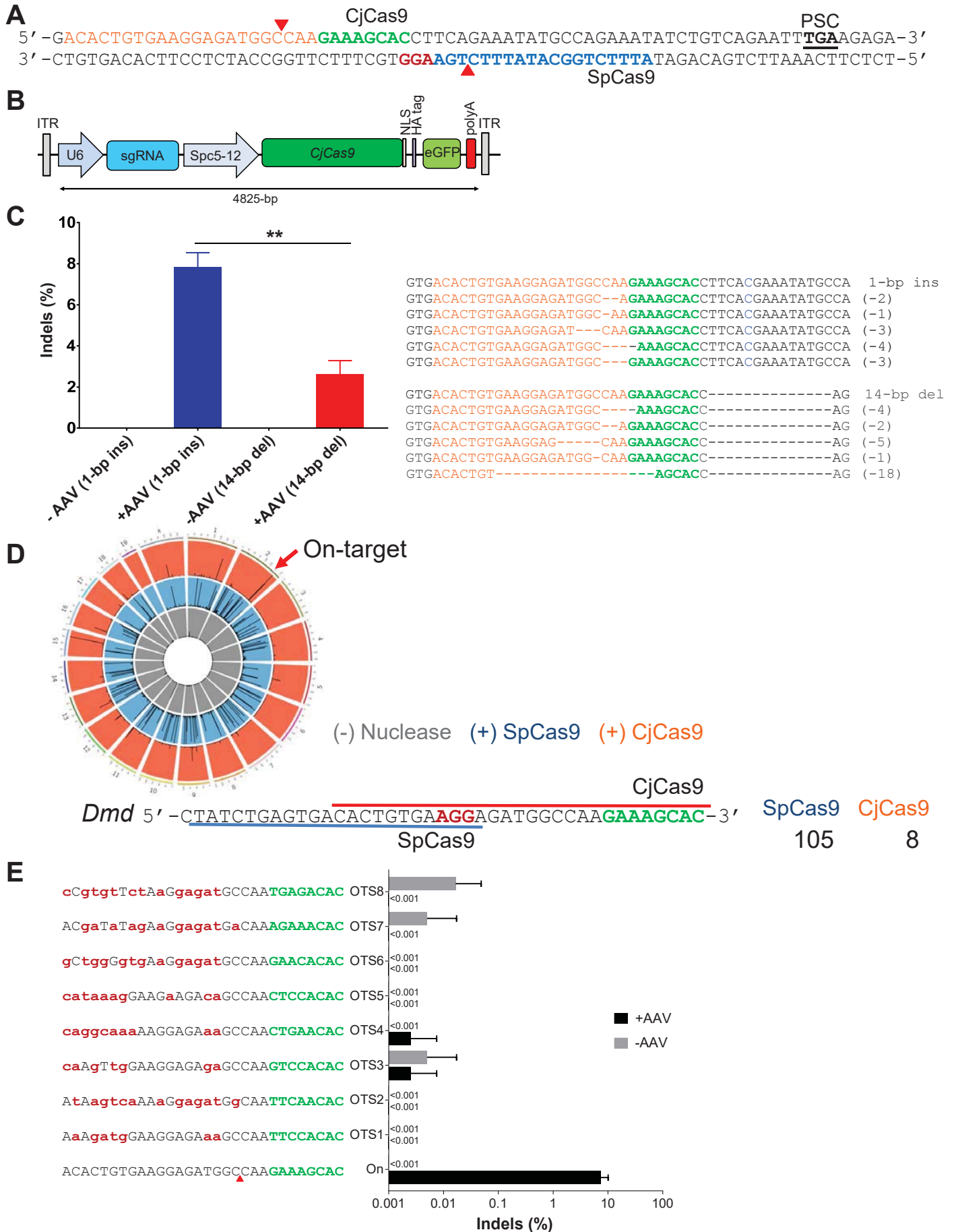-AAV (gray)

Indels (%)

Figure 3
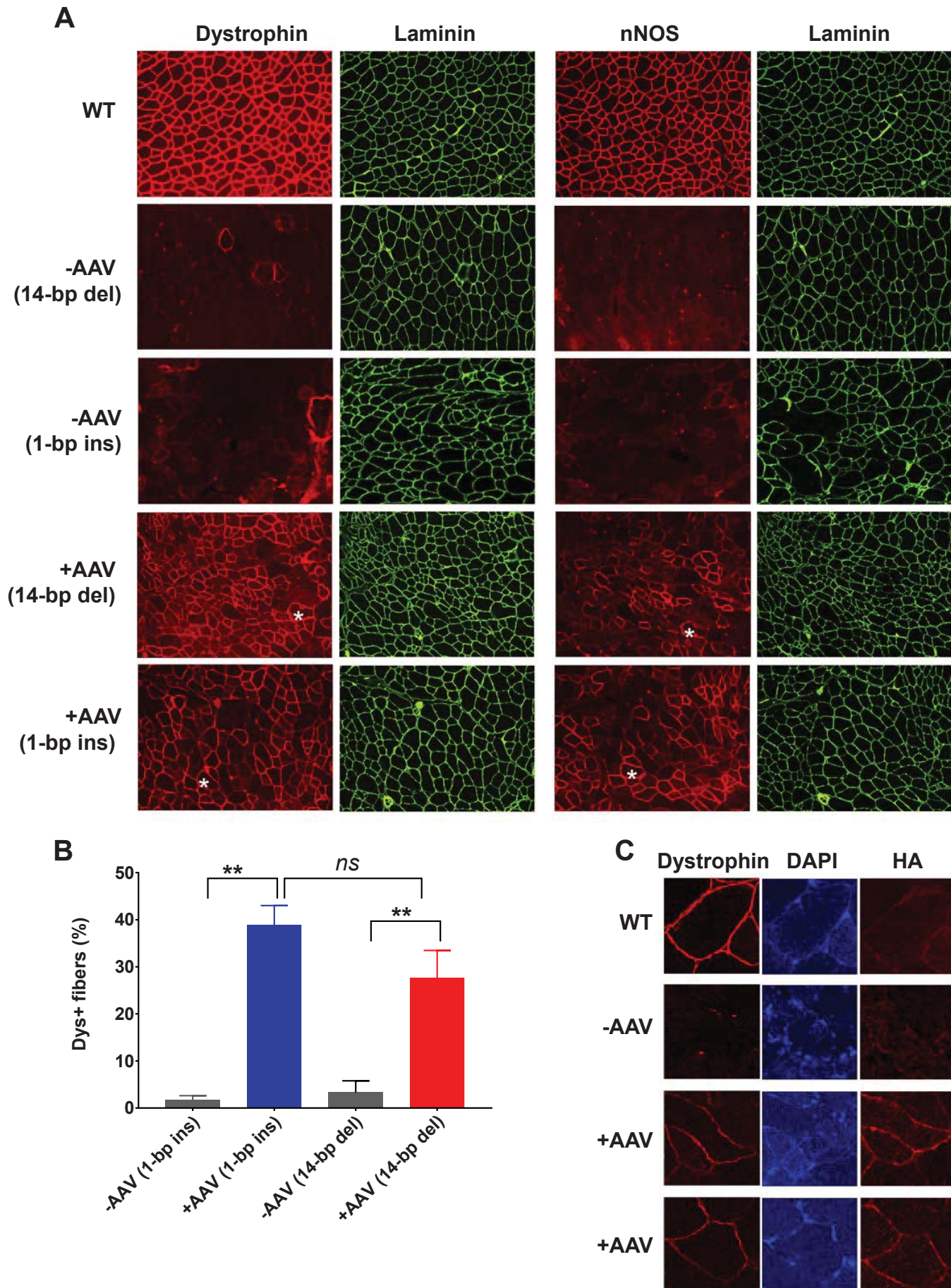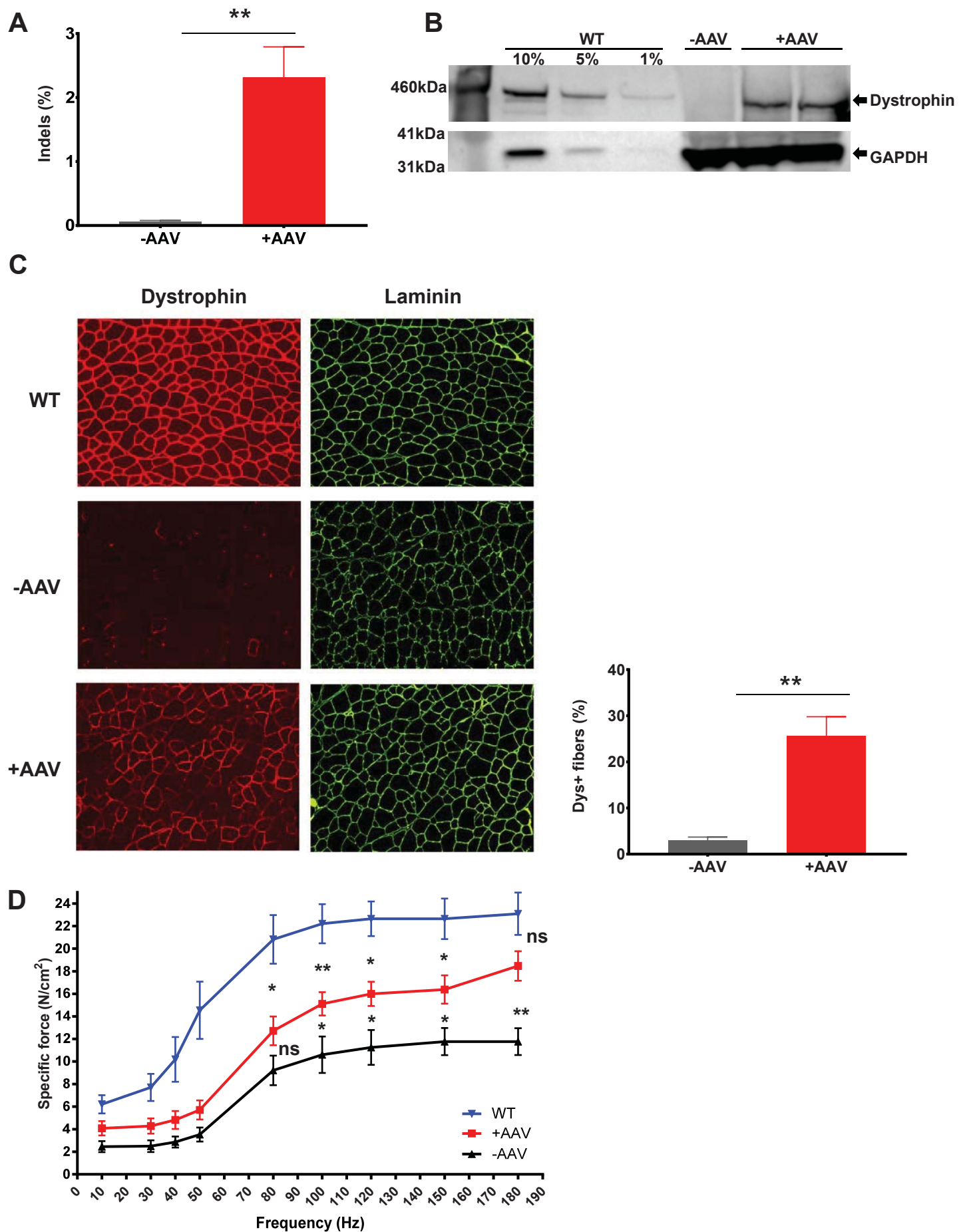
A

B

C

Figure 4

eTOC synopsis

Koo et al. demonstrate that CjCas9 derived from *Campylobacter jejuni* can be used as a gene editing tool to correct an out-of-frame *Dmd* exon in *Dmd* knockout mice. This study provides the therapeutic utility of CjCas9 for the treatment of Duchenne muscular dystrophy and other neuromuscular diseases.